

Spectral density characteristics of self-organized structuring in phase-synchronized oscillator ensembles

Magnus F Ivarsen*

Department of Physics and Engineering Physics, University of Saskatchewan, Saskatoon, Canada

Self-organized turbulence represents a way for structuring in nature to arise through sheer complexity rather than through linear instability theory. Simulating ensembles of oscillators that undergo phase synchronization through a propagating Kuramoto-interaction field, we present the spectral characteristics of spontaneous, self-organized structures of locally coupled oscillators. We demonstrate that the spectral density of emergent structures can exhibit universal scaling laws, in line with expectations from nature, indicating that observed statistical outcomes of complex physical interactions can be achieved through a more general principle of self-organization. We suggest that spontaneously generated structures may provide nuance to the reigning reductionist explanations for the observed structure in coupled systems of astrophysical and geophysical plasmas.

I. INTRODUCTION

When a smooth, laminar flow begins to break up into swirling, counter-streaming, and mixing parcels, the flow is said to be *turbulent*. Mathematically, such complex, composite motions are subject to Fourier analysis, which reveals that specific modes of fluctuation within the medium couple non-linearly, transferring energy from larger to smaller scales. The manifold interactions involved in non-linear mode coupling constitute coupled systems of stochastic processes, and the ordered complexity of the greater system can be subject to statistical mechanics and emergence.

In general, emergence describes the appearance of novel properties and behaviors in complex systems that are not readily predictable from a study of the interactions governing their individual constituents [1]. In physics, the phenomenon involves a phase change and the macroscopic collapse of a symmetry that is retained by the statistical behaviour of the system's microscopic constituents [2].

Emergent phenomena abound in physics. High-temperature superconductivity exhibits a strong dependency on specific material qualities, and its very existence seem to emerge from the complex interaction of material constraints [3, 4]. In the same vein, observations of Efimov physics, quantum few-body systems, exhibit scaling properties that are emergent rather than universal [5]. Likewise, Earth's oceans see the emergence of "freakishly" tall ocean waves that are deemed impossible based on all available information. These are caused by the growth of certain modes, a resonance that far surpasses any likely outcome of non-linear mode-coupling, replicated both in controlled experiments [6] and in nature [7].

Common for the above well-studied instances of emergence is that they challenge a purely reductionist view of nature. To see why, we note that emergence is woven

into science itself. The study of smaller systems in isolation provides the foundation upon which the study of those systems in aggregate can rely. For example, biology emerges from the chemical interactions of condensed matter. The rising supremacy of statistical methods in fields such as psychology and economics have yielded the concrete sense that *certain phenomena can only be understood in terms of statistics*. For example, understanding the world's financial markets through the study of individual human actors is a futile endeavor; instead, understanding is gleaned from descriptive, statistical models.

The explanatory value of such explanations lie in their ability to predict universally observed characteristics, implying that collective interactions in many-body systems can generate seemingly universal macroscopic behavior. We will base this investigation of emergence in turbulence physics, specifically in the study of self-organized structuring in weakly interacting ensembles of oscillators [8], whose phases couple with a localized Kuramoto model [9]. These are systems of oscillators whose initial stochastic distribution in phase are synchronized by localized feedback loops; random tendencies for phase synchronization are amplified, aggregated, and further amplified [10]. For such systems, Ref. [11] demonstrated theoretically that when oscillators are coupled locally on a network with cycles, the system can support multiple distinct, stable phase-locked solutions.

In the present paper, we aim to demonstrate how such weakly coupled systems exhibit universal scaling laws. To this end, we have developed a numerical simulation of self-organized point-cloud structures that arise through a Kuramoto-like phase synchronization mechanism, governed by a local interaction field and an external driver. Based on a Monte Carlo-analysis of the simulation's outcomes, we quantify and measure the power spectral density characteristics of the emergent point-cloud structures, and we argue that the stable spectral indices that we observe are characteristic and likely universal to the dimensionality of the system. Spontaneously generated, dissipative, self-organized structuring may then enter into the present, reductionist explanations for turbulence observations in nature.

* Contact: magnus.fagernes@gmail.com; Also at The European Space Agency Centre for Earth Observation, Frascati, Italy

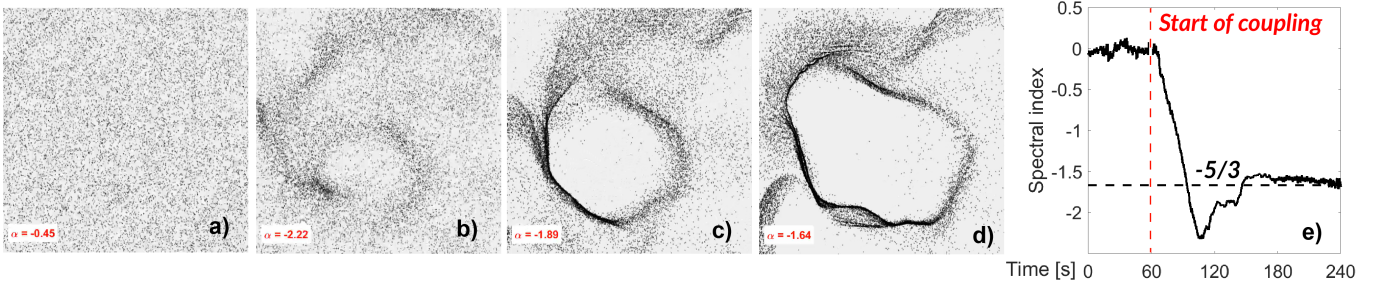


FIG. 1. **Panels a–d**): Four frames of Video S1, documenting a simulation of 30,000 oscillators subject to phase synchronization through a propagating Kuramoto-field, specified by a “pill box” kernel, demonstrating the emergence of a vortex. Panel e) shows the temporal development in α , the spectral index of the equivalent 2D Fourier transformed image, with the onset of coupling, as well as “Kolmogorov’s 5/3”, indicated.

II. METHODS

We simulated the time-evolution of ensembles of k oscillators, ϕ_k , defined as point sources whose velocity magnitude and direction are decided by their internal phase. Localized synchronization events are amplified and that amplification can drive ‘phase currents’ [11]. Figure 1, which represents Video S1 in the Supplementary Materials, shows this evolution from a symmetric chaos (panel a) to the emergence of dense propagating structures (panel d). Video S1 demonstrates how this principle leads to the spontaneous generation of a vortex.

In our simulations, emergence of asymmetric structures occurred through a locally propagating field, based on the Kuramoto model of coupled oscillators [12, 13]. Kuramoto synchronization is triggered by local, random alignments in phase, which get amplified by the interaction, leading to an instability [10, 11, 14]. The triggering of this instability leads to widespread phase synchronization and the collapse of the chaotic symmetry. The locality of the interaction, which differ from the conventional, global implementation of Kuramoto models, is produced by a propagating field equipped with a “pill box” kernel. The framework was motivated by a recent model of an active, excitable fluid system of interacting elements capable of self-organization (see Ref. [8], and references therein).

The simulation contains an ensemble of N oscillators in a two-dimensional domain with periodic boundary conditions. Each oscillator k is defined by its position vector $\mathbf{x}_k = (x_k, y_k)$ and an internal phase $\phi_k \in [0, 2\pi)$. The motion of each oscillator is decided by the phase,

$$\mathbf{v}_k(t) = v_0(\cos \phi_k(t)\mathbf{x} + \sin \phi_k(t)\mathbf{y}), \quad (1)$$

\mathbf{x}, \mathbf{y} being unit vectors. The initial state of the system is one of maximum entropy, with positions and phases drawn from uniform random distributions. Each oscillator is also assigned a constant natural frequency, ω_k , sampled from a physically-motivated, multi-slope power-law distribution intended to represent a broad spectrum of natural modes within the medium. Figure 2a shows

examples of these distributions, with “fast” and “slow” distributions in natural phase.

The spatiotemporal evolution of the simulation is thereafter driven by the iterative development in oscillator phase, where the central dynamic is produced by the Kuramoto model. The phase is updated at each time step Δt using a discretized form of a driven, stochastic Kuramoto-like equation:

$$\begin{aligned} \phi_k(t + \Delta t) = & \phi_k(t) + [\omega_k - \\ & - A_0 H(t) A_{\text{local}}(t) \sin(\phi_k(t) - \Psi_{\text{local}}(t)) + \xi_k(t)] \Delta t, \end{aligned} \quad (2)$$

where,

- ω_k is the oscillator’s intrinsic natural frequency, whose distribution follows a scaling law typical in real astrophysical or geophysical system of plasmas.
- $A_0 H(t)$ is the time-varying coupling strength, consisting of a base coupling strength A_0 and the Heaviside step function $H(t)$.
- $Z_{\text{local}}(t) = A_{\text{local}}(t)e^{i\Psi_{\text{local}}(t)}$ is the complex local mean field, representing the average phase and coherence of the oscillator’s neighbors.
- $\xi_k(t)$ is a Gaussian white noise term of a specified strength, representing stochastic fluctuations produced by the sum of influencing processes in a real astrophysical or geophysical system of plasmas.

The local mean field, a function of x and y , is calculated by binning the simulation space into a 64×64 -grid. At each step, the density is computed for each grid cell, and this field is then propagated via a 2D convolution with a circular averaging (“top-hat” or “pill box”) kernel. This models a sharp, local interaction within a fixed ‘interaction radius’, ensuring that phase information propagates with a finite range and speed, in accordance with expectations for field-perpendicular waves in astrophysical or geophysical plasmas.

Emergence occurs when initial inhomogeneities in the spatial distribution of phases are amplified and further

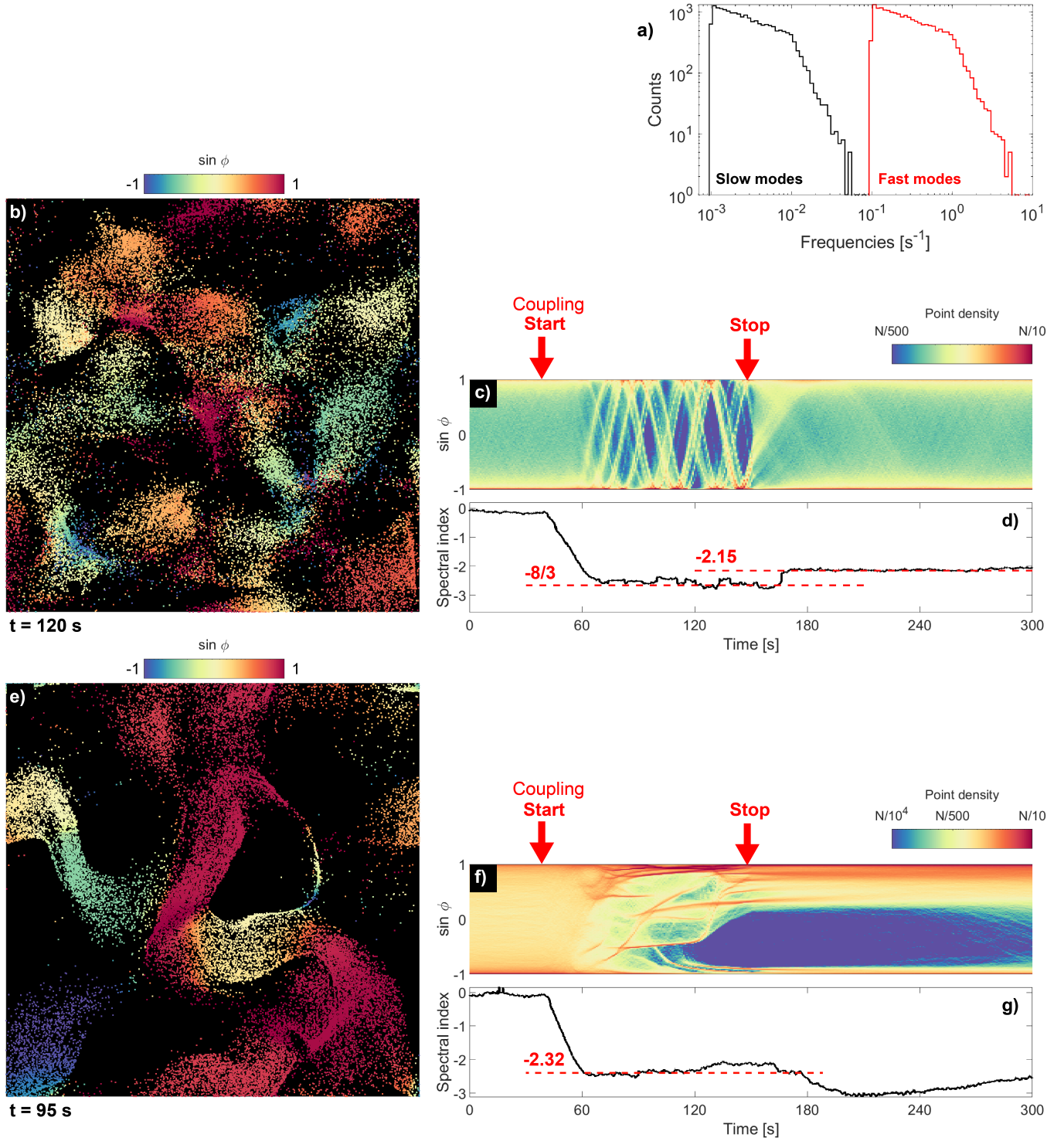


FIG. 2. **Panel a)**: The distribution in the oscillators' natural frequencies ω_k , for the convection-like slow modes (black) and the gyration-like fast modes (red). **Panels b) and e)** show snapshots of two simulations, using the fast and low modes respectively. The panels feature the spatial organization of the oscillator ensemble, with the sine of the phase shown with a colorscale. **Panels c) and f)** show a "time-phase-density" diagram of the two simulations, showing oscillator density with a colorscale, simulation time on the x -axis and the sine of the phase along the y -axis. **Panels d) and g)** show timeseries of the measured spectral slope for the two simulations, with stable values indicated. For videos of the events, see Videos S2 and S3 in the Supporting Materials.

amplified through a negative feedback between spatial clustering and phase synchronization, ultimately due to an alignment of the oscillators' velocities. The model therefore shares characteristics with models of milling bacteria, flocking birds, and schooling fish (the Vicsek model, e.g. [15, 16]). Unlike those models, ours relies on oscillator motion through phase changes. That said, the phases are scaled such as to facilitate the motion of the oscillators throughout the simulation space. Velocity alignment therefore provides a crucial feedback mechanism between phase coherence and spatial density.

To reiterate, the feedback mechanism is triggered by small, spontaneous regions of synchronization, which will cause oscillators to aggregate, having aligned their velocities. The resulting spatial clustering increases the local density, which in turn strengthens the local mean field, creating a non-linear feedback loop that drives the formation of large-scale, coherent structures.

The system is modeled as open and non-equilibrium. The coupling strength $\alpha(t)$ is controlled by a simple step-function driver, $A_{\text{drive}}(t)$. The driver is held at zero for the first third or fourth of the simulation's duration, allowing the system to remain in a symmetric, chaotic state, and then abruptly jumps to and holds a high value, an event that acts as the trigger for the non-equilibrium phase transition into a locally ordered, synchronized state.

Time-increments in the phase of each oscillator (Eq. 2) use a 4th order Runge-Kutta step for updating the phase (Eq. 2), and a simple Euler step for the positions,

$$\mathbf{x}_k(t + \Delta t) = \mathbf{x}_k(t) + \mathbf{v}_k(t)\Delta t. \quad (3)$$

Analysis and Output To quantify the emergent structures we extract key measurements from the simulation at each timestep. The 1D spatial power spectrum, $P(k)$, of the oscillator point-cloud is calculated using an efficient method based a 2D FFT, obtained on the images resulting from binning the oscillator locations onto a 2D 64×64 -grid. We then azimuthally average the resulting 2D power spectrum. We note that this spectrum is particular in that it reflects *spatial fluctuations in the density of oscillators* rather than oscillator phases.

To characterize the geometry of the emergent turbulence, or the statistical shape, the log-log power spectrum is fitted with a linear function, and we extract and store its slope, α . This is the spectral index, a staple in the research of astrophysical and geophysical plasmas and systems of plasmas [17–20]. Its value describes the continuous transfer of power, or energy, from larger to smaller scales, either in shallow (inertial), instability-driven regimes, or in steep dissipative, kinetic regimes [21–23].

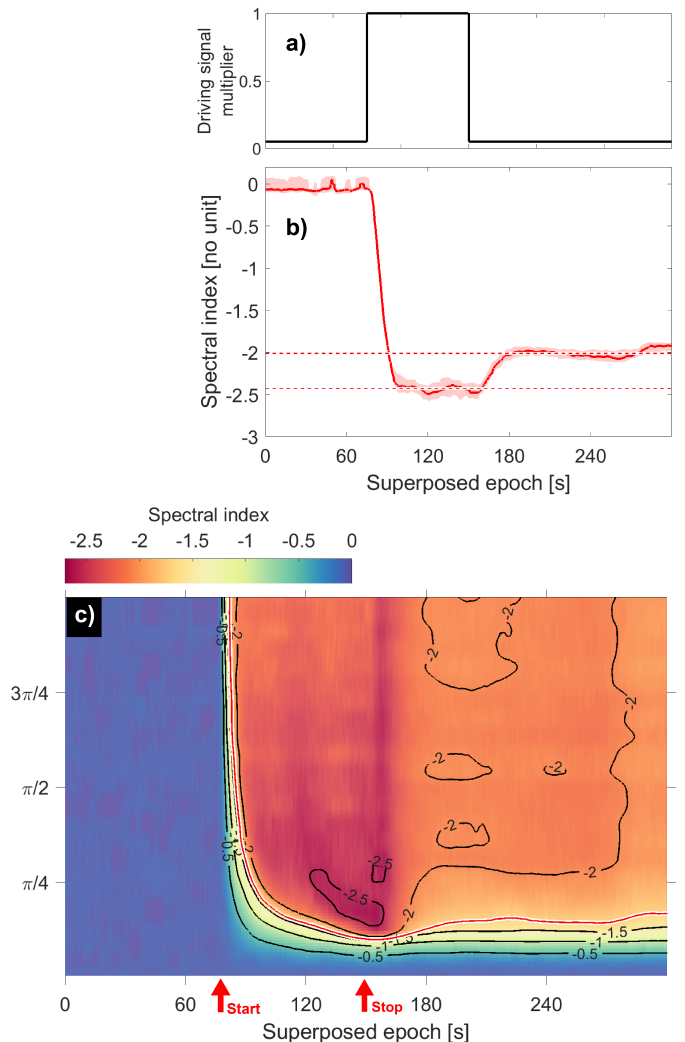


FIG. 3. **Panel b)** shows a superposed epoch analysis in spectral index of 24 iterations of the simulation, each with $N = 30,000$ oscillators, a base coupling strength of 1.1, interaction radius 3, and a “top hat” driving signal, itself shown in **panel a)**. Median spectral index is shown with a red line, with upper/lower quartile distributions are shown with a shaded pink region. Panel c) aggregates 24 superposed epoch analyses, with 24 Monte Carlo iterations within each. A color scale denotes spectral index, with selected contour lines of constant spectral index shown.

III. RESULTS

Figure 2 presents an analysis of the phase evolution in two different simulations; we simulate a “fast” oscillating mode (black distribution in Figure 2a), as well as a “slow” (red distribution in Figure 2a). Figure 2b) and e) show snapshots of the simulation space, with color representing the sine of the phase, showing how the fluctuations naturally scale by variation in phase. This phase is shown in a phase spectrogram with $\sin \phi_k$ on the y -axis and simulation time on the x -axis. The initiation and cessation of

the driving signal are indicated with black arrows. The measured spectral index values for the emergent shapes are shown in Figure 2d) and g).

The simulations in Figure 2 contain several interesting features. The fast-oscillating modes start in a chaotic, symmetric state. Upon emergence, the system cycles through a narrowly defined set of cycling modes, and when the signal is shut off a chaotic symmetry is restored to the system. Note that the ‘phase-velocity’ that we observe during the driving signal is equal to A_0 , which controls the speed with which the evolution in phase can develop. As to the spatial fluctuations corresponding to these developments in phase, we observe that the slow modes produce convection-like filaments whose oscillations amplitude is larger than the box. This should be contrasted against the “fast modes” (Figure 2a), whose oscillations are largely contained in the box. See Video S2 in the Supporting Materials for a video that substantiate our descriptions of the events.

Meanwhile, the spectral index, a mathematical description of the *shape* of the clustering point-clouds, shown in Figure 2d) and g), steepens with the breaking of the initial, chaotic phase symmetry. The spectral index stabilizes during the external driving signal at a value of -2.67 and -2.32 for the two simulations respectively. Then, the spectral index shallows for the fast “gyration-like” fluctuations in Figure 2b) (the fast modes), whereas is *steepens* for the slower “convection-like” fluctuations in Figure 2e) (the slow modes). This must be compared to the phases being largely symmetric at the end-state in Figure 2c), a symmetry that remains broken in Figure 2g).

Figure 3b) shows a superposed epoch analysis, elucidating the trends in spectral index that are triggered by oscillator synchronization, using fast distributions in the natural phase of the oscillator ensembles. This is obtained by taking the median and upper/lower quartile distributions of the a Monte Carlo ensemble for each timestep. Figure 3b) substantiates the spectral density behaviour seen in Figure 2g), with a stable emergent spectral index of around -2.5 while oscillator coupling is facilitated, settling onto the shallower value of -2 when the coupling subsides, and the oscillators are again in a symmetric, chaotic state.

Figure 3c) shows 24 such superposed epoch analyses, with a varying base coupling strength A_0 (along the y -axis); median spectral index is now shown with a colorscale. For base coupling strengths above a low threshold, then, we observe largely universal behaviour, although with somewhat steeper spectral indices for the lower base coupling strengths. The trigger for synchronization (or, equivalently, for spectral steepening) seems to lie around $A_0 = 0.44$.

Next, we repeat the Monte Carlo analysis for a external driving signal that does not subside (to elucidate the entirely driven system). Figure 4 shows the end result of two Monte Carlo aggregates, showing spectral index with a colorscale and contour lines as a visual aid, Fig-

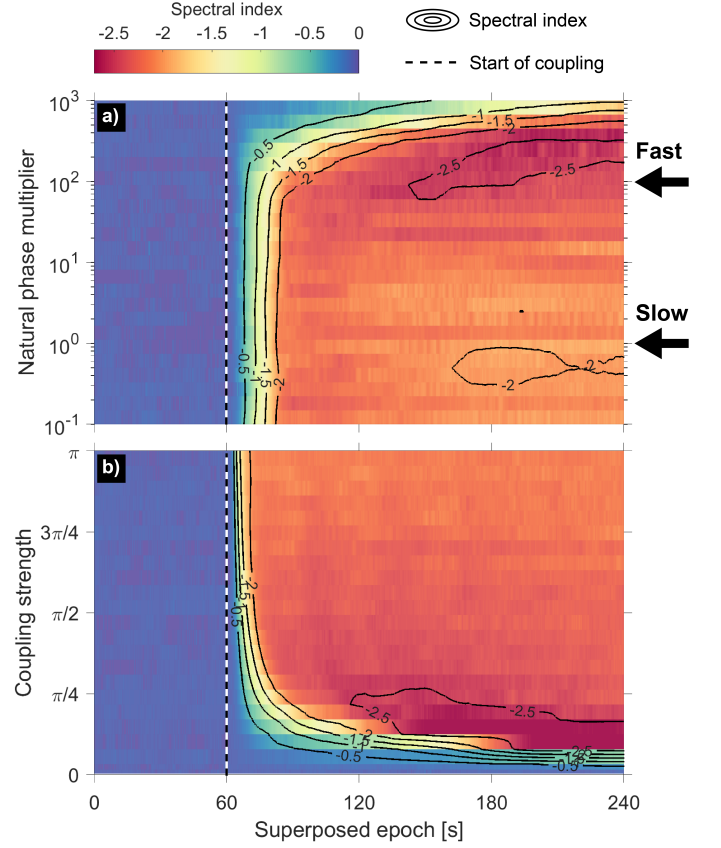


FIG. 4. The results of a Monte Carlo estimation of the average spectral indices seen in ensembles of self-organized, phase-synchronized oscillators subject to a local, propagating Kuramoto field. Superposed epoch denotes the progress of each simulation, where the coupling is initiated at the 60 s-mark. **Panel a)** shows a systematic variation in oscillator natural phase ω_k , taken as a multiplier of the distribution shown in Figure 2 (black distribution). **panel b)** shows the distinct “gyration-like” fast modes, now with base coupling strength A_0 in variation. For the simulations in Panel a), a base coupling strength was varied between 0.8 and 1.3,.

ure 4a) features a natural phase multiplier (distinguishing between the fast and slow natural modes) on the y -axis and superposed epoch on the x -axis, whereas Panel b) features base coupling strength A_0 on the y -axis.

In both aggregates, the spectral index quickly stabilizes on a value that is only weakly dependent on coupling strength, and somewhat dependent on the modes in the system; with the fast modes exhibiting steeper spectra than the slow modes. The stability with which the spectral index settles across the various considerations of the oscillator interactions leads us to consider that steep, dissipative spectral density is universal to self-organized ensembles of weakly coupled oscillators.

IV. DISCUSSION

We have simulated ensembles of oscillators that are subject to phase synchronization through a locally mediated Kuramoto interaction, demonstrating that complex structures emerge from relatively simple, localized interactions between locally coupled oscillators. This configuration builds on the theoretical foundation by Ref. [11]. We quantify the shape of these self-organized structures, appearing through clustered point-clouds of oscillators, through measurements of the spectral index, the logarithmic decay in power spectral density with increasing wavenumber. We have evaluated the spectral index during individual simulations (Figures 1, 2), superposed epoch analyses of several simulations (Figures 3 and 4). The results have been a powerful demonstration how self-organized structuring can emerge from coupled systems of oscillatory motions. We have characterized the dissipative nature of such emergent structuring, and the likely universality in steep spectral indices (with values roughly between -2 and -3). The macroscopic behavior seen in our simulations is robust and depends only on the macroscopic parameters.

The main result of the present paper is this apparent universality in the spectral indices that we observe in the simulations. Since similarly valued spectral indices are already widespread in astrophysical and geophysical observations, these results imply that, when a system features a sufficient number of coupled oscillations, the observed structuring of fields and matter in that system, or system of systems, may in part be self-organized [8], expressive of the dimensionality of the interactions rather than physical processes. This sweeping implication comes with the caveat that our simulations are synthetic, in that they do not reflect specific physical systems, and so our results must be substantiated in simulations that couple real, physical systems.

Whereas our simulated ensembles of oscillators are artificial, their characteristics are chosen so as to provide a foundation for understanding the origin of structure in

astrophysical and geophysical systems of plasmas, where oscillatory modes are ubiquitous and directly linked to turbulent structuring [24–28]. Our results demonstrate that oscillator-based self-organized structures adhere to characteristic and perhaps universal spectral index values that are in line with expectations for plasma turbulence: observations in space consistently yield an index value roughly between -3 and -1.5 for electrostatic turbulence [23, 28–30]. In particular, the -8/3 value which seems to be favoured for the ensembles of weakly coupled, fast oscillators (Figures 3c and 4a) is associated with kinetic-scale magnetohydrodynamic turbulence [31]. This is in direct support of a recent preprint, Ref. [28], which proposes that self-organized structuring is a viable explanation for auroral plasma turbulence in Earth’s ionosphere, and is motivated by observations of plasma structuring that is directly driven by wave-particle interactions [26, 27].

It is, again, important to point out that our observations cannot be taken into account for any specific system of coupled plasmas. The results are entirely independent of the Vlasov equation for many-body systems under long-range force interaction and the governing principles of magnetohydrodynamics. However, in this precise point lies the versatility of our results: by essentially recreating the spectral characteristics of well-known turbulent phenomena, we show that spectral density scaling laws can be universal.

Here, we note that the principle of synchronization through velocity alignment is fundamental to a range of systems, such as milling animals, schooling fish, and flocking birds. The present paper demonstrates that synchronized alignment through coupled oscillations is a viable way to recreate turbulent “behaviour” that is currently observed in tenuous space plasmas. The very cacophony of the ionosphere, where both mechanical and electromagnetic waves abound and are subject to instability and field-perpendicular coupling, lends credibility in emergence as a potentially fundamental cause of structuring in the auroral ionosphere.

-
- [1] R. C. Bishop, *The Physics of Emergence (Second Edition)* (IOP Publishing, 2024).
 - [2] R. B. Laughlin, *A Different Universe: Reinventing Physics from the Bottom Down* (Basic Books, New York, 2005).
 - [3] B. Keimer, S. A. Kivelson, M. R. Norman, S. Uchida, and J. Zaanen, High Temperature Superconductivity in the Cuprates (2014), arXiv:1409.4673 [cond-mat].
 - [4] A. Bussmann-Holder and H. Keller, High-temperature superconductors: Underlying physics and applications, *Zeitschrift für Naturforschung B* **75**, 3 (2020).
 - [5] R. Schmidt, S. Rath, and W. Zwerger, Efimov physics beyond universality, *The European Physical Journal B* **85**, 386 (2012).
 - [6] K. Trulsen, H. Zeng, and O. Gramstad, Laboratory evidence of freak waves provoked by non-uniform bathymetry, *Physics of Fluids* **24**, 097101 (2012).
 - [7] D. Chalikov, Freak waves: Their occurrence and probability, *Physics of Fluids* **21**, 076602 (2009).
 - [8] M. Y. Marov and A. V. Kolesnichenko, Self-Organization of Developed Turbulence and Formation Mechanisms of Coherent Structures, in *Turbulence and Self-Organization: Modeling Astrophysical Objects*, edited by M. Y. Marov and A. V. Kolesnichenko (Springer, New York, NY, 2013) pp. 373–423.
 - [9] J. A. Acebrón, L. L. Bonilla, C. J. Pérez Vicente, F. Ritort, and R. Spigler, The Kuramoto model: A simple paradigm for synchronization phenomena, *Reviews of Modern Physics* **77**, 137 (2005).
 - [10] S.-Y. Ha and S.-Y. Ryoo, Asymptotic Phase-Locking Dy-

- namics and Critical Coupling Strength for the Kuramoto Model, *Communications in Mathematical Physics* **377**, 811 (2020).
- [11] R. Delabays, T. Coletta, and P. Jacquod, Multistability of phase-locking and topological winding numbers in locally coupled Kuramoto models on single-loop networks, *Journal of Mathematical Physics* **57** (2016).
 - [12] S.-Y. Ha, H. K. Kim, and S.-Y. Ryoo, Emergence of phase-locked states for the Kuramoto model in a large coupling regime, *Communications in Mathematical Sciences* **14**, 1073 (2016).
 - [13] R. E. Mirollo and S. H. Strogatz, The spectrum of the locked state for the Kuramoto model of coupled oscillators, *Physica D: Nonlinear Phenomena* **205**, 249 (2005).
 - [14] R. Mirollo and S. Strogatz, The Spectrum of the Partially Locked State for the Kuramoto Model, *Journal of Nonlinear Science* **17**, 309 (2007).
 - [15] A. Costanzo and C. K. Hemelrijk, Spontaneous emergence of milling (vortex state) in a Vicsek-like model, *Journal of Physics D: Applied Physics* **51**, 134004 (2018).
 - [16] S.-Q. He, Z. Chang, D. Liang, C.-H. Li, Q.-L. Liang, X. Yin, and G.-K. Xu, A self-enhanced mobility mechanism drives the spontaneous emergence and transformation of vortex patterns, *Soft Matter* **21**, 6627 (2025).
 - [17] Kivanc and R. A. Heelis, Spatial distribution of ionospheric plasma and field structures in the high-latitude F region, *Journal of Geophysical Research* **103**, 6955 (1998).
 - [18] J. Safránková, Z. Němeček, F. Němec, L. Přech, C. H. K. Chen, and G. N. Zastenker, Power Spectral Density of Fluctuations of Bulk and Thermal Speeds in the Solar Wind, *The Astrophysical Journal* **825**, 121 (2016).
 - [19] K. Song, A. M. Hamza, P. T. Jayachandran, K. Meziane, and A. Kashcheyev, Spectral Characteristics of Phase Fluctuations at High Latitude, *Journal of Geophysical Research: Space Physics* **128**, e2022JA031244 (2023).
 - [20] M. F. Ivarsen, Y. Jin, A. Spicher, and L. B. N. Clausen, Direct Evidence for the Dissipation of Small-Scale Ionospheric Plasma Structures by a Conductive E Region, *Journal of Geophysical Research: Space Physics* **124**, 2935 (2019).
 - [21] H. Mounir, A. Berthelier, J. C. Cerisier, D. Lagoutte, and C. Beghin, The small-scale turbulent structure of the high latitude ionosphere - Arcad-Aureol-3 observations, *Annales Geophysicae* **9**, 725 (1991).
 - [22] A. Spicher, W. J. Miloch, L. B. N. Clausen, and J. I. Moen, Plasma turbulence and coherent structures in the polar cap observed by the ICI-2 sounding rocket, *Journal of Geophysical Research: Space Physics* **120**, 2015JA021634 (2015).
 - [23] M. F. Ivarsen, J.-P. St-Maurice, Y. Jin, J. Park, W. Miloch, A. Spicher, Y.-S. Kwak, and L. B. N. Clausen, Steepening Plasma Density Spectra in the Ionosphere: The Crucial Role Played by a Strong E-Region, *Journal of Geophysical Research: Space Physics* **126**, e2021JA029401 (2021).
 - [24] K. Rinnert, Plasma waves observed in the auroral E-region - ROSE campaign, *Journal of Atmospheric and Terrestrial Physics* **54**, 683 (1992).
 - [25] M. F. Ivarsen, M. D. Gillies, D. R. Huyghebaert, J.-P. St-Maurice, A. Lozinsky, D. Galeschuk, E. Donovan, and G. C. Hussey, Turbulence Embedded Into the Ionosphere by Electromagnetic Waves, *Journal of Geophysical Research: Space Physics* **129**, e2023JA032310 (2024).
 - [26] Y. Shen, O. P. Verkhoglyadova, A. Artemyev, M. D. Hartinger, V. Angelopoulos, X. Shi, and Y. Zou, Magnetospheric Control of Ionospheric TEC Perturbations via Whistler-Mode and ULF Waves, *AGU Advances* **5**, e2024AV001302 (2024).
 - [27] M. F. Ivarsen, Y. Miyashita, J.-P. St-Maurice, G. C. Hussey, B. Pitzel, D. Galeschuk, S. Marei, R. B. Horne, Y. Kasahara, S. Matsuda, S. Kasahara, K. Keika, Y. Miyoshi, K. Yamamoto, A. Shinbori, D. R. Huyghebaert, A. Matsuoka, S. Yokota, and F. Tsuchiya, Characteristic E-Region Plasma Signature of Magnetospheric Wave-Particle Interactions, *Physical Review Letters* **134**, 145201 (2025).
 - [28] M. F. Ivarsen, K. Song, L. Spogli, J.-P. St-Maurice, B. Pitzel, S. Marei, D. R. Huyghebaert, S. Kasahara, K. Keika, Y. Miyoshi, Y. Kazama, S.-Y. Wang, A. Matsuoka, I. Shinohara, S. Yokota, P. T. Jayachandran, and G. C. Hussey, The Origin of Structure in the Auroral Ionosphere (2025), arXiv:2507.11755 [physics].
 - [29] M. F. Ivarsen, J.-P. St-Maurice, Y. Jin, J. Park, L. M. Buschman, and L. B. Clausen, To what degree does the high-energy aurora destroy F-region irregularities?, *Frontiers in Astronomy and Space Sciences* **11**, 10.3389/fspas.2024.1309136 (2024).
 - [30] M. F. Ivarsen, J.-P. St-Maurice, G. Hussey, A. Spicher, Y. Jin, A. Lozinsky, L. V. Goodwin, D. Galeschuk, J. Park, and L. B. N. Clausen, Measuring small-scale plasma irregularities in the high-latitude E- and F-regions simultaneously, *Scientific Reports* **13**, 11579 (2023).
 - [31] V. David and S. Galtier, $k_{\perp}^{-8/3}$ Spectrum in Kinetic Alfvén Wave Turbulence: Implications for the Solar Wind, *The Astrophysical Journal Letters* **880**, L10 (2019).